Br_2 Production from the Heterogeneous Reaction of Gas-Phase OH with Aqueous Salt Solutions: Impacts of Acidity, Halide Concentration, and Organic Surfactants

Elizabeth K. Frinak[†] and Jonathan P. D. Abbatt*

Department of Chemistry, 80 Saint George Street, University of Toronto, Toronto, Ontario M5S 3H6, Canada

Received: May 23, 2006; In Final Form: July 17, 2006

This study reports the first laboratory measurement of gas-phase Br_2 production from the reaction between gas-phase hydroxyl radicals and aqueous salt solutions. Experiments were conducted at 269 K in a rotating wetted-wall flow tube coupled to a chemical-ionization mass spectrometer for analysis of gas-phase components. From both pure NaBr solutions and mixed NaCl/NaBr solutions, the amount of Br_2 released was found to increase with increasing acidity, whereas it was found to vary little with increasing concentration of bromide ions in the sample. For mixed NaCl/NaBr solutions, Br_2 was formed preferentially over Cl_2 unless the Br^- levels in the solution were significantly depleted by OH oxidation, at which point Cl_2 formation was observed. Presence of a surfactant in solution, sodium dodecyl sulfate, significantly suppressed the formation of Br_2; this is the first indication that an organic surfactant can affect the rate of interfacial mass transfer of OH to an aqueous surface. The OH-mediated oxidation of bromide may serve as a source of active bromine in the troposphere and contribute to the subsequent destruction of ozone that proceeds in marine-influenced regions of the troposphere.

1. Introduction

Modeling studies and field measurements have shown ozone depletion near the Earth's surface can be positively correlated to elevated concentrations of inorganic bromine.[1−7] This relationship is strongly demonstrated in the Arctic springtime boundary layer and in regions close to salt lakes at lower latitudes. O_3 depletion in the overall marine boundary layer may also be occurring, but at levels that are harder to observationally quantify.

There are now well-established mechanisms by which gas-phase, free-radical bromine catalytically destroys O_3;[7] it is known that autocatalytic release of active bromine can occur from sea salt via the uptake of HOBr;[3,5] and there is a viable mechanism for the recycling of active bromine once it is formed.[8,9] Of particular note is that depletions in the amount of bromide, relative to the ratio of bromide to sodium in seawater, have been reported in snow and aerosol samples in the Arctic as well as lower latitudes.[10−13] Also, measurements by Newberg et al.[10] show that bromide was depleted even in marine aerosol with low anthropogenic influence. The reported depletions were most significant in the size fraction < 1.6 μm, which corresponded to the fraction with the highest acidity. These results are indicative of bromine release and cycling in the troposphere, but the initial processes responsible for liberating the bromine from these surfaces remain poorly quantified in either absolute or relative terms.

There are a number of candidates for this initiation process, each of which may prevail under different environmental conditions. Gas-phase photolysis of organobromine compounds has generally been considered to be too slow, in particular for the case of bromoform. Instead, most schemes focus on sea salt as the original source of gas-phase bromine, in the form of concentrated brines, frozen seawater, frost flowers, marine aerosol, or snow upon which aerosol has deposited. Through both experiments and models, possible gas−surface interactions that have been identified so far include ozone-mediated release of Br_2 on frozen seawater and aqueous sodium bromide solutions,[14] NO_x–bromide interactions,[15] interactions of HSO_5^- with bromide,[16] and, last, the interactions of hydroxyl radical formed either photochemically in the particle[17−19] or taken up from the gas phase.[18,20] Of all these, only the chemistry involving gas-phase hydroxyl radical has not been experimentally examined, largely because of the particularly difficult nature of the experiments.

This study builds upon previous work involving bromide oxidation via the generation of aqueous OH, produced either through photolysis of dissolved nitrate or nitrite or by pulsed radiolysis.[17−19,21,22] In particular, the work of Zafiriou[19] is pivotal in pointing out that condensed-phase OH is believed to preferentially oxidize bromide over chloride in seawater solutions. However, the question we address in this paper is different because the oxidative processes involving OH and bromide will occur at the interface of the solutions under study, as discussed later. In particular, although OH is known to be taken up efficiently by aqueous solutions,[23] it has yet to be shown that such interfacial processes will lead to bromide oxidation; instead, existing experimental studies in the literature have only focused on bulk chemistry arising from the *in situ* production of OH within the aqueous samples.[17−19,21,22] The likelihood of significant surficial chemistry comes from a suite of modeling studies that show that halide anions and hydroxyl radicals have a strong affinity for the surface.[24−27]

The atmospheric motivation for the specific focus on OH as an initiator for Br_2 release comes from the observation that BrO formation in the boundary layer is usually associated with sunrise, either on a diurnal scale, as in the Dead Sea region, or seasonally, as in the Arctic. Whether this dependence arises only because the autocatalytic cycle involving HOBr uptake is driven

* To whom correspondence should be addressed. Phone: (416) 946-7358. E-mail: jabbatt@chem.utoronto.ca.
† Present address: University of New Hampshire, Durham, NH.

10.1021/jp063165o CCC: $33.50
Published on Web 08/17/2006

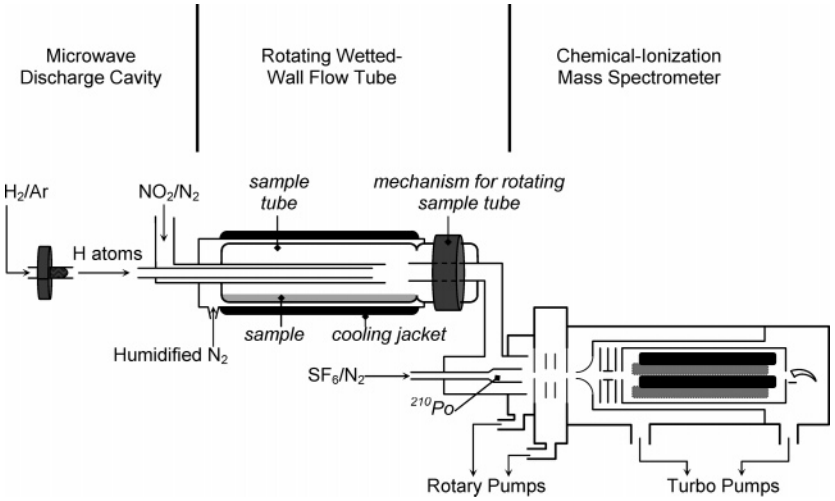

Figure 1. Schematic of the experimental apparatus.

TABLE 1: Molar Concentrations of Salt Samples and the Corresponding Abbreviation Used in the Text

[NaBr]	[NaCl]	abbreviation
3.9	<0.02	CSB
4.9×10^{-3}	3.4	SWSB
2.5×10^{-4}	3.4	DSB

by sunlight or whether the initiation step also requires sunlight is not known. However, it is known that dark processes alone are not able to provide sufficient levels of active bromine to destroy ozone in their own right.

In this paper we seek to answer the following questions: Is gas-phase bromine formed from the interaction of gas-phase OH with solutions containing bromide? If so, what is the yield of Br_2 formed relative to OH lost? What is the dependence of the production rate on the acidity, bromide content, and chloride content of the solutions? And what is the impact of an organic surfactant present in the solution upon the Br_2 production rate?

2. Experimental Section

Experiments were conducted in a horizontally oriented, rotating, wetted-wall flow tube shown schematically in Figure 1, which is similar to a flow reactor described previously in the literature.[28] To characterize the influence of concentration of bromine production, samples of varying bromide concentrations were prepared. The most concentrated samples were 3.9 M NaBr (Sigma-Aldrich, 99.0%), abbreviated in the text as CSB (concentrated sodium bromide). The most dilute samples were 3.4 M NaCl (ACP Chemicals, 99.0%), which contained an impurity of 2.5×10^{-4} M NaBr as reported by the manufacturer. These samples will be referred to as DSB (dilute sodium bromide) in the text. Samples were also prepared containing a $[Cl^-]$:$[Br^-]$ molar ratio of approximately 700:1, which is similar to the ratio of 620:1 found in seawater. Samples of this concentration will be condensed to SWSB (seawater sodium bromide) within this text. Table 1 provides a summary of the sample concentrations in units of moles per liter with the corresponding abbreviations. The acidity was increased using H_2SO_4 (Fisher, 96.0%), and the pH of the solutions measured using an Orion 520A pH meter calibrated using buffers at pH 1.00, 4.00, and 7.00.

Following preparation, a 3 mL aliquot of salt solution was placed in the glass sample insert (1.5 cm i.d., by 30 cm length) in the flow tube as indicated by the gray shaded area in the center section of Figure 1. The sample insert effectively acts as the flow volume within a fixed flow tube. The Teflon tube conveying the gas-phase components to the chemical-ionization mass spectrometer (CIMS) also does not rotate. The purpose of rotating the sample insert was to minimize exposed glass surface within the flow tube and to replenish the sample surface with bromide as it is oxidized away. The entire glass sample insert rotated during experiments at a speed of approximately 10 revolutions per minute (rpm). A uniform sample coating was attained by rinsing the glass insert with a 5% solution of HF and with water, prior to conducting an experiment. The solution was confined by a ridge in the glass insert to the cold region within the flow tube. The temperature of the sample was held at 269 K using a Neslab LT50 low-temperature bath circulator by flowing chilled ethylene glycol through the cooling jacket. The temperature of the flow tube was calibrated using a copper−constantan thermocouple. A humidified flow of 1100−1600 cm^3(STP) min^{-1} N_2 combined with 100−250 cm^3(STP) min^{-1} Ar sustained a relative humidity (RH) of approximately 78% with respect to liquid water at 269 K to ensure samples remained in the aqueous phase. For reference, the deliquescence RHs of NaCl and NaBr are 75 and 58%, respectively.[29,30] The corresponding bulk flow velocity ranged between 93 and 143 cm/s. We estimate the relative change in composition of the solution by either uptake or loss of water vapor is only 0.03%/min. This slow rate of change is expected to have a negligible impact on the experiments in this study.

The schematic in Figure 1 is divided into three sections labeled microwave discharge cavity, rotating wetted-wall flow tube, and CIMS. The first region highlights the precursors for the hydroxyl radicals. OH was formed from the following reaction:

$$H + NO_2 \rightarrow OH + NO \qquad (1)$$

Using an MKS flow controller, 105−250 cm^3(STP) min^{-1} argon (BOC Gases, UHP) containing trace amounts of hydrogen gas (BOC Gases, UHP) was flowed through a Beenakker microwave discharge cavity. The resulting hydrogen atoms were conveyed into the flow tube through a Teflon tube of 0.318 cm o.d. and 107 cm length. A 3.4 L glass bulb attached to a manifold contained a mixture of approximately 70:1 N_2 (BOC Gases, UHP):NO_2 (Matheson). The manifold terminated in a metering valve which delivered the N_2:NO_2 mixture into a 0.635 cm o.d. Teflon tube connected to the moveable glass injector tube, also

of 0.635 cm o.d. Given the concentrations used and the speed of reaction 1, the NO_2 then reacted with the hydrogen atoms per reaction 1 to rapidly form OH at the tip of the injector rod. Experiments were carried out in two different modes—one in which NO_2 was the limiting reagent and one in which NO_2 was present in excess—for reasons to be discussed below.

During experiments, the glass injector rod was pulled back to expose OH to the aqueous salt solution in the rotating wetted-wall flow tube. Any resulting gas-phase products, as well as the reactants, were carried downstream of the flow tube and monitored using CIMS. SF_6^- was chosen as the reagent ion because it enabled us to monitor NO_2, OH, Br_2, and Cl_2 simultaneously.[31,32] In particular, a trace amount of SF_6 (Scott Specialty Gases, 99.99%) was carried in an N_2 flow through a radioactive polonium source (^{210}Po) to generate SF_6^- reagent ions. The ion source region is described in detail elsewhere.[33] The total N_2 flow through the ion source region was 10.5 sLm. After reaction of the species of interest with the SF_6^- reagent ion, ions continued to a declustering region in the mass spectrometer, followed by mass selection in a quadrupole and finally detection with a Channeltron electron multiplier operated in a single negative ion counting mode. Again, further details of the system may be found in Thornton et al.[33]

Calibrations of the NO_2 and Br_2 signals were performed to convert the resulting CIMS count rates, reported as counts per second (cps), into concentrations. For both species, the concentration was quantified by measuring the change in pressure in the manifold over time. When OH was formed with NO_2 as the limiting reagent, the OH concentration was determined by the change in the NO_2 signal between when the Beenakker microwave cavity discharge was on and off. This quantification of OH represents an upper limit as it was assumed the entire suppression in the NO_2 signal was due to a 1:1 conversion of NO_2 to OH. The Br_2 signal was calibrated in a similar manner as the NO_2 signal using a 3.4 L bulb filled containing approximately 300:1 N_2:Br_2. Gas-phase Br_2 was transferred from a 100 mL bulb containing liquid bromine (ACP Chemicals) after successive freeze−pump−thaw cycles into a 3.4 L bulb where it was mixed with N_2.

Detection limits for NO_2 and Br_2 were 9.6×10^{10} and 5.6×10^{10} molecules/cm^3, respectively, for an integration time of 30 s and a $S/N = 1$. Note that these detection limits were compromised to a significant degree by our decision to detect OH, Br_2, NO_2, and Cl_2 simultaneously through the use of the SF_6^- as the reagent ion. In particular, SF_6^- is known to react with water vapor.[34] To maintain reasonable detection limits and roughly 50 000 cps of reagent ion signal, we operated the flow tube at a sufficiently low temperature, 269 K, that the water vapor effect was not overwhelming. Similarly, since the goal of the experiment was not to measure uptake coefficients of OH to the solutions, the pressure in the flow tube was kept reasonably high, 94 Torr, where the CIMS gives the best sensitivity but plug flow conditions do not prevail. Typical OH starting concentrations were quite high, with an upper limit of 2×10^{12} molecules/cm^3.

A typical experiment consisted of adding a 3 mL sample to the system and cooling it to 269 K over a period of 2 h. The flow tube was then opened to a mechanical pump, and the flows of humidified N_2, Ar, and the CIMS N_2 were established. The relative humidity of the system was typically 78% with respect to liquid water with the pressure in the flow tube at about 94 Torr as measured by a Baratron capacitance manometer. Then the system was opened to the declustering, mass selection, and detection regions of the mass spectrometer. Upon establishing constant signals of SF_6, NO_2, and OH with the glass sample insert rotating, the samples were exposed to OH. In the mode with NO_2 as the limiting reagent, the injector tube was pulled back, incrementally exposing the sample at a rate of 2 cm every 10 min. When NO_2 was present in excess, the injector was retracted in one step, exposing the entire 29 cm of sample.

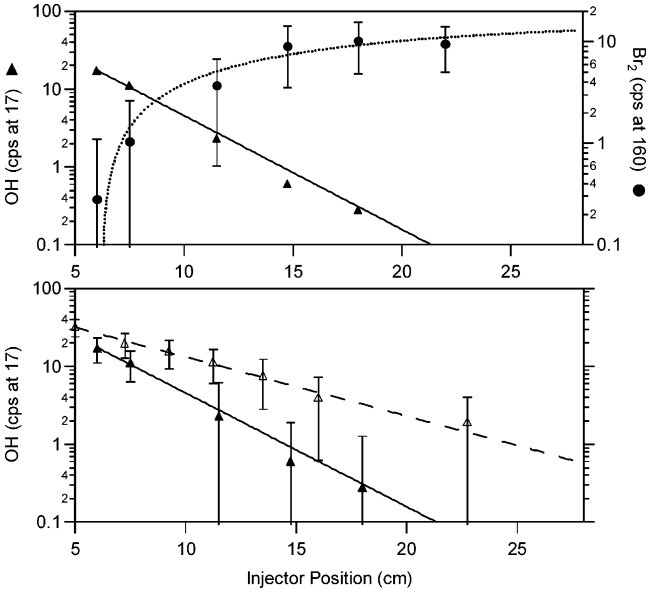

Figure 2. (Top panel) Correlation between Br_2 production (●, dotted line, right axis) and OH loss (▲, solid line, left axis) as a function of injector position during a typical experiment. The data shown are for a CSB sample of pH 0.5. (Bottom panel) Comparison of OH loss on CSB at pH 5.4 (△, dashed line) and pH 0.5 (▲, solid line). Bars for bromine in the top panel and for OH in the bottom panel represent the standard deviation in the averaged signal at the corresponding injector position.

3. Results

The principal qualitative observation reported in this paper is that gas-phase Br_2 formation occurs when OH is exposed to bromide-containing solutions, providing they are sufficiently acidic. The top panel of Figure 2 illustrates typical behavior where the loss of OH signal is plotted coincident with the formation of Br_2. This particular experiment is for Br_2 production from 3 mL of a CSB sample of pH 0.5. Injector distance correlates to the length of sample exposed to OH. The OH signal shown is the count rate as monitored at a mass-to-charge ratio of 17, and the Br_2 signal is shown in the same units as those detected at a mass-to-charge ratio of 160. Fits to the data are single-exponential decay and growth, respectively. SWSB samples of pH 0.5 were also characterized using this method and exhibited similar behavior. This is direct experimental evidence that molecular bromine can be formed by the heterogeneous interaction of gas-phase OH with halide solutions. It should be noted that blank experiments were conducted to ensure the Br_2 signal was due to reaction with OH. These experiments consisted of exposing samples with the microwave off but with H_2 and NO_2 flowing, or in the absence of NO_2 but with the microwave on. In both cases, no Br_2 was measured. In addition, one SWSB experiment was performed with HCl acidification in place of H_2SO_4. Br_2 formation was observed, indicating that the oxidation chemistry was not being initiated by the reaction of OH with HSO_4^-.

In the bottom panel of Figure 2 is the OH decay rate on a pH 5.4, CSB solution. This behavior is consistent in replicate measurements. Clearly, the decay is significantly slower with

the high-pH sample, and there is no observed Br_2 formation. Care should be taken in interpreting kinetic behavior from the curves because the conditions were not in the plug flow regime; that is, the role of gas-phase diffusion and mixing in this experiment are sufficiently undefined at the relatively high pressures of the flow tube therefore dominating over the kinetics of the gas−surface interaction. In particular, turbulent mixing may be an important factor in the transportation of OH to the wall. Nevertheless, it is clear that OH is not lost on solutions near neutral pH as efficiently as on acidic solutions than would occur if molecular diffusion was the only mixing process.

Quantitatively, experiments were conducted to determine the bromine yield, defined as the concentration of Br_2 produced divided by the concentration of OH initially present. Using a method from gas-phase, free-radical, flow-tube kinetics studies,[35] these experiments were done with H atoms in excess. Experimentally, we could verify that NO_2 was the limiting reagent by observing the NO_2 signal dropping from roughly 30 cps to very close to zero cps when the microwave discharge containing H_2 was switched on. As previously mentioned in the Experimental Section, the quantification of OH strictly represents the upper limit to the concentration. However, given the response of the NO_2 signal to the addition of H_2, we believe that the vast majority of the change in the NO_2 signal gives rise to OH formation.

A second issue related to the calculation of the Br_2 yield is whether the OH formed all reacts on the surface of the solution or whether it can decay away to some degree in the gas phase also. The gas-phase reactions of potential importance include the following:

$$OH + NO_2 + M \rightarrow HNO_3 + M \quad (2)$$

$$OH + NO + M \rightarrow HONO + M \quad (3)$$

$$OH + OH \rightarrow H_2O + O \quad (4)$$

$$OH + OH + M \rightarrow H_2O_2 + M \quad (5)$$

$$OH + Br_2 \rightarrow HOBr + Br \quad (6)$$

The observed first-order rate constant for OH loss on the acidic solution in Figure 2 is on the order of 44 $s^{-1,}$ which is significantly greater than the estimates of the rate constants for reactions 2−5 at the point of addition of OH to the flow tube. However, reaction 6 between OH and Br_2 requires further consideration. We estimate the importance of this reaction using a simple numerical model that includes OH loss at the wall giving rise to 0.5 Br_2 molecules per OH molecule lost and gas-phase reaction of OH with Br_2.[36] We find that 84% of the overall OH loss of 44 s^{-1} is due to reaction with aqueous bromide to produce Br_2 with the remainder arising from subsequent reaction directly with Br_2. And so, we feel confident that the primary loss process for OH is indeed via reaction with the aqueous surface and that the difference in reactivity on the acidic and neutral solutions is mainly due to additional OH reactivity on the former.

The results for the bromine yield experiments at pH 0.5 are 0.3 ± 0.1 for SWSB and 0.7 ± 0.5 for CSB samples. The uncertainty is one standard deviation for precision only for four and five replicate experiments, respectively. For the reasons outlined above, we consider these to be lower limits to the bromine yields. An additional factor that arises in this regard is that Br_2 yields can be suppressed to some degree by reaction 6 with OH. For the data in Figure 2, we estimate using the numerical model described above that this effect is on the order of about 30% loss.

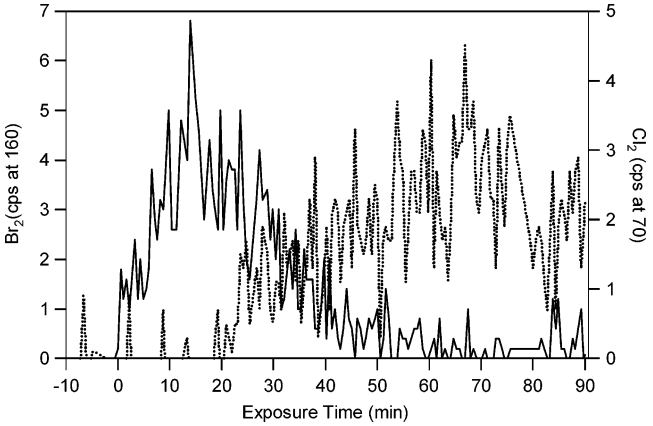

Figure 3. Transition from Br_2 production (solid line, left axis) to Cl_2 production (dotted line, right axis) in a sample of CSB at pH 0.5.

Figure 3 shows data from the exposure to OH of a DSB sample at pH 0.5. For comparison, the $[Cl^-]$:$[Br^-]$ molar ratio in this solution was 13 600:1. In this experiment OH was produced with NO_2 as the limiting reagent. However, the injector rod was pulled back in one step, exposing the entire 29 cm of sample at once. The data show that despite the very large excess of chloride ions, Br_2 is evolved before Cl_2. Only after the Br_2 signal has peaked and begun to decrease does the Cl_2 peak grow in, illustrating the extreme preference oxidants have for bromide over chloride in solution. As discussed in more detail in section 4.1 (Reaction Mechanism), this observation is consistent with both the proposed surface segregation of bromide ions[24−27] and the known bulk chemistry.[37,38] During this experiment we looked for gas-phase BrCl production but saw no signal above the CIMS detector noise.

The second class of experiments involved measuring the Br_2 production rate as a function of solution acidity and bromide content. Given experimental considerations, we chose to perform these experiments with NO_2 in excess; the NO_2 signal would decrease when the microwave discharge was switched from off to on, but not to zero. The reason for this transition was that the conditions in excess H were hard to achieve, being dependent on the somewhat variable H-atom output of the discharge. Instead, we found that much more reproducible conditions were maintained between runs using excess NO_2. Slight variations in the conditions were quantitatively accounted for as described below.

Figure 4 summarizes the Br_2 concentrations formed from exposure to a nominally constant amount of OH, in experiments performed with NO_2 in excess at a concentration of roughly 1 × 10^{13} molecules/cm^3. The concentration of Br_2 produced is shown as a function of pH. The fit is a single exponential to guide the eye for CSB samples, but similar trends are seen for the samples of lower bromide concentrations as denoted by the other symbols. Though the DSB samples exhibit slightly less Br_2 production, there is no detectable difference between the more concentrated samples. Each data point represents an average of results conducted from roughly four replicate experiments, and the error bars indicate the standard deviation of those measurements. Though Br_2 was never measured in samples of pH 5.4, it is possible that Br_2 was released at a concentration below the instrumental limit of detection of 5.6 × 10^{10} molecules/cm^3. The main point to note is that Br_2 production increases dramatically with increasing acidity but does not depend as strongly on bromide concentration.

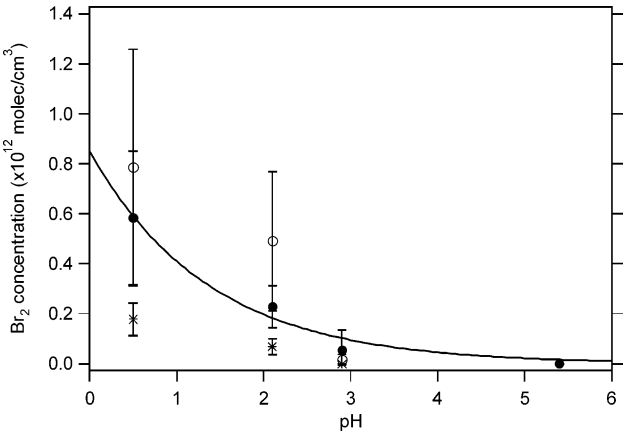

Figure 4. Variation in Br_2 production as a function of pH. Markers correspond to CSB (●), SWSB (○), and DSB (∗). Bars indicate standard deviation determined from replicate measurements. Curve is a single-exponential fit to CSB data to guide the eye.

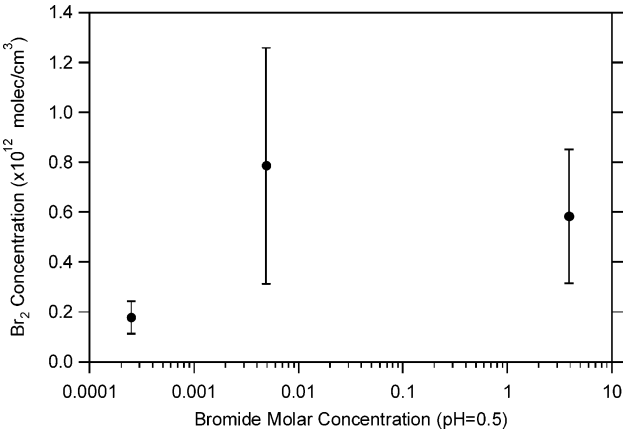

Figure 5. Variation in Br_2 production as a function of bromide concentration. Data shown are for samples of pH 0.5. Bars indicate standard deviation from replicate measurements.

Figure 5 depicts the variation in Br_2 production with bromide concentration in samples of pH 0.5. The concentration of Br_2 is somewhat reduced in the DSB samples, but given the 4 orders of magnitude change in the bromide concentrations, there is remarkably little difference between the bromide production rates for the solutions studied. The results clearly show that a sample with a similar chloride-to-bromide ratio as seawater yields the same quantity of Br_2 as a sample highly concentrated in bromide.

For all of the data in Figures 4 and 5, the experiments were conducted under nominally the same conditions, with NO_2 in excess, constant flow conditions, and roughly the same flow rate of H_2 through the microwave discharge. However, given that the production rate of H atoms may have varied from experiment to experiment, the change in NO_2 signal with the microwave discharge on and off was noted for each experiment. We used this information to normalize the bromine signals for variable OH production rates in each experiment; the OH signal itself was not used in this regard because of variable wall loss of OH in the Teflon tube connecting the flow tube to the CIMS. Similarly, because the overall CIMS sensitivity also varied to some degree from experiment to experiment, either due to the slow decay of the ^{210}Po source or due to variable SF_6 flow rates, the sensitivity of the instrument to NO_2 was measured for each experiment. This was achieved using the CIMS signal for NO_2, as measured with the microwave discharge off, and from the concentration of NO_2 in the flow tube, as calculated from the pressure decrease with time of the manifold connected to the NO_2 reservoir.

Finally, given the possibility that organic films may reside on the surface of marine particles,[39,40] we attempted to observe formation of Br_2 from pH 0.5, DSB solutions with variable concentrations of a common surfactant, sodium dodecyl sulfate (SDS), present. These solutions reproducibly yield $(4 \pm 2) \times 10^{16}$ molecules of Br_2 during 20 min of exposure to OH without the SDS present. The reported uncertainty is the standard deviation for five replicate measurements. However, the maximum Br_2 level observed was $12 \pm 3\%$ of this value when SDS concentrations were varied over 2 orders of magnitude from 0.18 to 2 mM. The low value of this concentration range is close to the critical micelle concentration,[41] although full data on this quantity are not available for the properties of our solutions at the temperature and pH of the experiments. Nevertheless, we feel confident in saying that the SDS is able to significantly hinder the production of bromine, most probably because OH reacts instead with the surfactant layer present on the solution surface.

4. Discussion

4.1. Reaction Mechanism. The chemistry of OH in bulk sodium bromide solutions has been studied in the laboratory previously through early work involving the pulsed radiolysis technique and more recently by investigations involving photolysis of dissolved OH precursors such as nitrate or hydrogen peroxide[17−19,21,22] as well as modeling studies.[42] Oxidation is initiated by the reaction of OH with bromide, which proceeds at approximately the diffusion-controlled rate:[38]

$$Br^- + OH \leftrightarrow HOBr^- \quad (7)$$

$HOBr^-$ can either dissociate to re-form Br^- and OH, react with a proton to form Br, or react with Br^- to form Br_2^-:

$$HOBr^- + H^+ \rightarrow Br + H_2O \quad (8)$$

$$HOBr^- + Br^- \rightarrow OH^- + Br_2^- \quad (9)$$

Reactions 8 and 9 are keys because both ultimately lead to Br_2 formation via rapid chemistry:

$$Br + Br^- \leftrightarrow Br_2^- \quad (10)$$

$$Br_2^- + Br_2^- \leftrightarrow Br_3^- + Br^- \quad (11)$$

$$Br_3^- \leftrightarrow Br_2 + Br^- \quad (12)$$

Thus, the overall reaction for formation of Br_2 from OH is

$$2OH + 2Br^- + 2H^+ \rightarrow Br_2 + 2H_2O \quad (13)$$

where it is seen that protons are needed for reaction. We see that the bromine yields of 0.3 ± 0.1 for SWSB and 0.7 ± 0.5 for CSB samples measured for the most acidic solutions are consistent with the overall stoichiometry of reaction 13.

For the specific reaction between OH and the pure CSB, we first consider whether the chemistry will occur at the solution interface or not. Assuming for the time being that there is no preferential segregation of bromide ions to the surface, the reactodiffusive length for OH in the solution is calculated to be extremely short, only 1.5 Å, suggestive of a surface interaction:[43]

$$L = \left(\frac{D}{k^{I}}\right)^{0.5} = \left(\frac{D}{k^{II}[Br^-]}\right)^{0.5} \quad (14)$$

where we have used a bulk-aqueous-phase diffusion constant of 1×10^{-5} cm^2/s, a bulk concentration of 3.9 M Br^-, and the literature rate constant of 1.1×10^{10} M^{-1} s^{-1} for reaction 7. Considering that both bromide and OH are believed to partition to the surface of solutions,[24−27] we are even more confident that OH will interact with Br^- at the surface, forming $HOBr^-$. This conclusion is consistent with molecular dynamics studies by Roeselova et al.[25] that predict frequent interactions between surface adsorbed hydroxyl and halide anions.

To evaluate the subsequent chemistry, we apply the steady-state approximation to the concentration of $HOBr^-$ in the above chemistry, assuming bulk processes prevail. In particular, we can write an expression proportional to the rate of formation of oxidized bromine:

$$\text{rate} = \left[\frac{(k_8[H^+] + k_9[Br^-])}{k_{-7} + k_8[H^+] + k_9[Br^-]}\right] k_7[OH][Br^-] \quad (15)$$

For experimental concentrations and literature rate constants,[38,44] the quantity within the large brackets in eq 15 has a negligible pH dependence, as depicted in Figure 6 by crosses on the right-hand vertical axis. The reason for this trend is that reaction 9 proceeds sufficiently fast at high bromide concentrations that a rapid route for Br_2^- formation remains at all pH values. Whereas this expression is consistent with the pH dependence for bromide oxidation observed in previous kinetics studies,[21,22] we note these past studies were not performed with such high bromide concentrations as in our CSB solutions. However, if we assume that reaction 9 does not proceed, than the quantity in the brackets displays a distinct pH dependence, shown as open circles in Figure 6.

While it is true that the rate constants used to model the solution kinetics are those for room temperature and measurements were performed at 269 K, the temperature dependence for such fast ionic processes is usually quite weak. Instead, we propose the apparent absence of the fast reaction between $HOBr^-$ and Br^- is an indication that the chemistry occurring in the bulk does not prevail in the same manner at the interfaces of this solution. One possibility is that cations and anions are strongly associated with each other in this high ionic strength environment, perhaps in the form of contact-ion pairs. And so, it is more likely for the transient $HOBr^-$ species to interact with a hydrated proton at the surface, via the surface equivalent of reaction 8, than with a bromide ion as in (9). This suggestion is supported by recent surface spectroscopy studies that indicate protons are also preferentially found at the surface of halide solutions.[45]

A previous study has proposed a halogen production surface mechanism that proceeds without the involvement of a proton. Specifically, Oum et al.[14] observe formation of Cl_2 during the 254 nm photolysis of aqueous sodium chloride particles, O_3, and water vapor. Given the strong dependence of our Br_2 production rates on acidity, we see no evidence within our detection limits that indicates an analogous process occurs with bromine.

A final point we make concerning the acidity dependence is that the decreased yield of bromine at high pH is consistent with the decreased loss rate for OH shown in the bottom panel of Figure 2. Apparently, if the transient $HOBr^-$ surficial species cannot find a proton to react with, it dissociates and releases OH back to the gas phase. Another point to consider is that the relatively high fluxes of OH to the solution surfaces are removing protons faster than they are able to diffuse from the bulk to replenish those lost to reaction. In this manner it may be true that at the lower OH concentrations in the atmosphere, the acidity dependence displayed in Figure 4 will not be as strong.

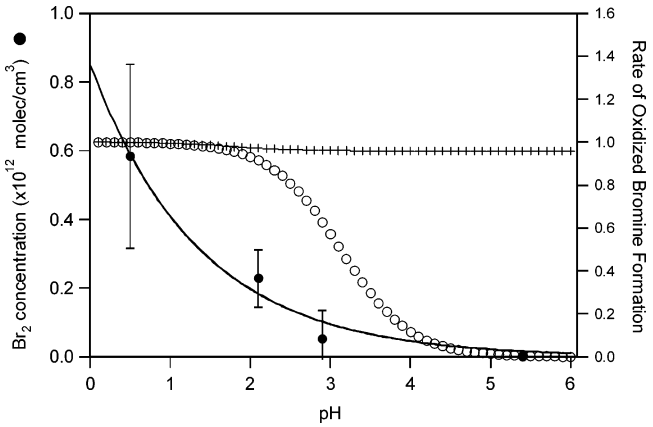

Figure 6. Measured variation in Br_2 production as a function of bromide concentration for samples of pH 0.5 as shown as closed circles (●) on the left axis compared to the modeled rate of oxidized bromine formation on the right axis. Crosses (+) represent a production mechanism that incorporates reaction 9 between $HOBr^-$ and Br^-, whereas the open circles (○) represent a mechanism that does not include reaction 9. See section 4.1 (Reaction Mechanism) for details. The right axis is a dimensionless value for the normalized rate of oxidized bromine formation.

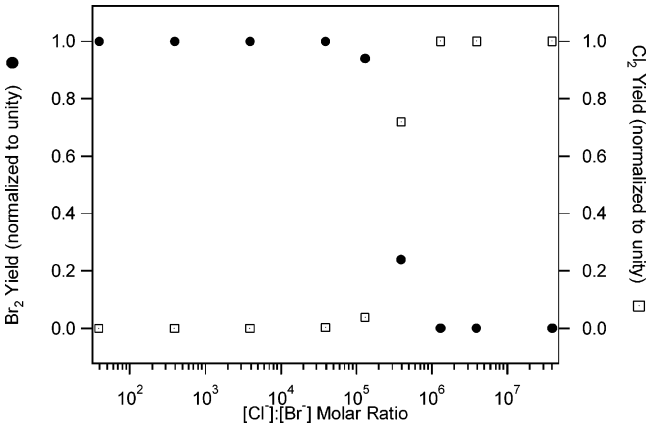

Figure 7. Plot of normalized yields of both Br_2 (●) and Cl_2 (□) as a function of the bromide concentration from a numerical model simulation of the aqueous-phase chemistry. The model was initialized with $[Cl^-] = 3.9$ M, $[H^+] = 0.32$ M (pH = 0.5), and $[OH] = 10^{-6}$ M, and run for 100 s. Room-temperature rate constants were taken from those referenced in the text and from Ershov et al.[37] In the model, OH initially interacts with Cl^-, given its high relative concentration, but Cl_2 is only produced in high yield after the $[Cl^-]$:$[Br^-]$ ratio exceeds 3×10^5. For reference, the value of this ratio in seawater is 620:1.

Turning now to the solutions that contain trace amounts of sodium bromide in concentrated sodium chloride, the primary findings are that the bromine yield and the bromine production rates are similar for the pure CSB solutions, despite orders of magnitude less bromide in solution. This indicates a very strong preference for oxidation of bromide over chloride at the interface, as indicated in earlier work by Zafiriou.[19]

It is reasonable to ask whether the chemistry is necessarily the same in the pure bromide solutions as in the mixed chloride/bromide solutions. In particular, again assuming for the time being that bulk chemistry prevails and that there is no

preferential concentration of bromide at the surface relative to chloride, one would expect that the incoming OH would much more likely interact with a chloride ion than a bromide ion:

$$OH + Cl^- \leftrightarrow HOCl^- \quad (16)$$

We suggest this because reaction 16 proceeds at the same diffusion-controlled rate as does reaction 7, but the concentration of chloride will be much higher than bromide. Similarly, one would expect that $HOCl^-$ would then react with a proton according to the diffusion-limited reaction 17,

$$HOCl^- + H^+ \rightarrow H_2O + Cl \quad (17)$$

but not with chloride given the very slow rate constant for reaction 18:[46]

$$HOCl^- + Cl^- \rightarrow Cl_2 + H_2O \quad (18)$$

Once the Cl atom is formed from reaction 17, it will complex with Cl^- to form Cl_2^-, again via a very fast reaction:

$$Cl^- + Cl \rightarrow Cl_2^- \quad (19)$$

At this point, a competition arises between processes that might give rise to gaseous Cl_2 production or gaseous Br_2 production, represented by the following reactions. In particular, Cl_2 can form via

$$Cl_2^- + Cl_2^- \rightarrow Cl_3^- + Cl^- \quad (20)$$

$$Cl_3^- \leftrightarrow Cl_2 + Cl^- \quad (21)$$

Via a set of very fast reactions, Cl_2^- can also initiate the oxidation of Br^- to either Br_2^- or Br, which ultimately will lead to Br_2 formation:

$$Cl_2^- + Br^- \rightarrow ClBr^- + Cl^- \quad (22)$$

$$ClBr^- + Br^- \rightarrow Br_2^- + Cl^- \quad (24)$$

$$ClBr^- \rightarrow Cl^- + Br \quad (24)$$

In a simple numerical model using the above chemistry as well as additional, less important reactions listed in Ershov et al.,[37] we have compared the relative rates of formation of Cl_2 to those of Br_2 formation in a mixed salt solution of 3.9 M NaCl and varying NaBr concentrations from an initial quantity of dissolved OH. The results are plotted in Figure 7 as a function of the molar concentration ratio in solution. It is seen that there is a very strong preference for the oxidation of bromide rather than chloride, all the way down to a concentration of roughly 10^{-5} M Br^- which corresponds to a $[Cl^-]$:$[Br^-]$ molar ratio on the order of 3×10^5.

Thus, bulk chemistry alone can explain the results displayed in Figure 3, where we see molecular bromine formed in preference to chlorine for the DSB solutions with only impurity levels of sodium bromide present. Similarly, we see from Figure 3 that molecular chlorine is only formed by exposure to OH once bromide is depleted in solution. Indeed, we estimate that roughly 4.5×10^{17} bromide ions are present in the solution exposed to OH. To within uncertainties, this is equal to the flux of OH to the surface during 25 min of exposure time for the experiment in Figure 3, assuming all OH present in the flow tube at a concentration of 2×10^{12} molecules/cm^3 is lost on the surface during this time. We saw no production of gas-phase BrCl which may be due to dissolved BrCl being readily converted to Br_2, rapid loss of $ClBr^-$ via reaction 24, or a lower sensitivity of the CIMS to BrCl.

Although bulk-phase chemistry can explain the preference for oxidation of bromide over chloride with OH, another intriguing possibility is that the bulk-phase model just presented is not correct. Given that bromide might partition to the surface preferentially over chloride, it is also possible that the chemistry is not initiated by reaction of OH with Cl^- but instead with Br^-. In this case the subsequent chemistry would then more closely resemble that described above for the pure sodium bromide solutions. The relative rates of the two mechanisms may be better discerned when experimental measurements of the ratio of chloride to bromide at the surface of a mixed sodium halide solution are available. At this point, we can only say that our observations are consistent with both bulk-phase and surface-phase chemistry; thus we feel no need to introduce new chemical pathways to explain the data.

4.2. Surfactant-Coated Solutions. We believe the observation that the SDS surfactant substantially reduces the Br_2 production rate is direct experimental evidence that organic monolayers can affect the uptake of OH by aqueous aerosol surfaces. It is likely that a reaction is occurring between OH and the SDS surfactant, as was experimentally demonstrated by Cooper and Abbatt,[47] where the loss of OH on solid ammonium sulfate surfaces was shown to be enhanced when exposed to a surfactant, 1-hexanol. It is also consistent with the later study of Bertram et al.[31] that demonstrated that OH readily reacts with a number of organic surfaces. In addition to recent laboratory measurements of N_2O_5 aqueous aerosol kinetics from our laboratory and others,[48−50] where the loss rate of gas-phase N_2O_5 is suppressed with organic surfactants such as humic substances, SDS, and hexanoic acid present in the aerosol, we believe this result provides additional evidence that organic surface layers can have a major impact on the rates of gas−surface chemistry that may occur in the atmosphere.

4.3. Atmospheric Implications. To assess the potential atmospheric importance of the chemistry we have observed, we can summarize by noting that the low level of bromide present in marine aerosol does not disfavor the production of bromine relative to chlorine with high yields, even for dilute bromide solutions. Although it is true that we only observe bromine production from a pH of approximately 3 or below, there is likely to be some bromine production at higher pH with yields below the detection limit of our experiment. It is also possible that the decreased yield at higher pH was due to depletion of protons at the surface of the solution due to the relatively high OH fluxes used in this work. At the lower OH concentrations in the atmosphere the yield may remain high under less acidic conditions.

However, given that a proton is clearly involved in the oxidation, it is most likely that the OH-mediated release of bromine will be important on acidic marine particles such as those that have experienced significant levels of pollution including HNO_3 or SO_2. Particles in the remote marine boundary layer also have their pH lowered from the value prevailing in ocean water by the aqueous-phase oxidation of background SO_2, but the rate at which this occurs and the degree of resultant acidity is generally lower than in the polluted case.

As indirect support of the pH dependence of bromine activation processes in general, we can consider a study by Tas et al.,[4] where the formation of bromine oxide (BrO) was monitored over the Dead Sea. Production of BrO was found to

vary diurnally, as expected, with the concentrations exceeding the instrumental limit of detection at the earliest around 2 h after sunrise. In particular, the concentration of BrO was found to increase with decreasing pH of the Dead Sea water. Also, the delay between sunrise and the appearance of measurable amounts of BrO increases with increasing pH. The results from this study suggest that the mechanism for Br_2 production is pH-dependent, as expected with OH−bromide oxidation chemistry, as well as with the HOBr-mediated autocatalytic cycle.

To be more quantitative, it will be important to compare the rate of this chemistry to that of other potential bromide activation processes, such as the heterogeneous uptake of gas-phase N_2O_5, NO_3, or O_3, plus the condensed-phase processes involving photolysis of nitrate in solution (to form OH) and the oxidation of bromide by HSO_5^-. For example, Hunt et al.[51] have investigated the heterogeneous reaction of O_3 with deliquesced NaBr aerosol. Upon extrapolation to atmospheric conditions, they concluded this reaction may serve as a source of between 0.003 and 22 ppt Br_2 in 10 h of darkness, with the range determined by how their experiments on pure sodium bromide particles are extrapolated to seawater composition.

For comparison, we can do an initial calculation to illustrate the potential importance of OH-mediated bromine release. The calculation that follows is similar to those of Matthew et al.[18] and Herrmann et al.,[20] which both also claim that this chemistry may represent an important source of active bromine. We use the same marine aerosol volume loading of 6.3×10^{-11} cm^3/cm^3 as that employed by Sander and Crutzen,[3] which was in turn used by Matthew et al.[18] and Herrmann et al.[20] For a monodisperse distribution of particles with radius 1.5×10^{-4} cm, this corresponds to 4.5 particles/cm^3 and a total aerosol surface area of 1.3×10^{-6} cm^2/cm^3. For particles of this size at atmospheric pressure, there is a significant gas-phase diffusion mass-transfer limitation, with the resistances to uptake and diffusion being comparable to each other for uptake coefficients of roughly 0.1. And so, for the calculations below we use an uptake coefficient of 0.05 for two reasons. One, there will not be much limitation to mass transfer by gas-phase diffusion for this value. Two, assuming that the uptake coefficient is unity in our work at pH = 0.5 and, as described above, that the decrease in the Br_2 yield as a function of pH is due to a smaller uptake coefficient, we estimate the value on the pH 2.9 solutions to be roughly 0.05.

And so

$$\text{rate of oxidized Br production} = \frac{[\text{OH}]_g \gamma \upsilon A}{4} \qquad (25)$$

where υ is the mean molecular speed, A is the surface area of aerosol per unit volume of air, and γ is the reactive uptake coefficient. For an OH concentration of 2×10^6 molecules/cm^3, the yield of oxidized bromine using the values mentioned above is $2.0 \times 10^3/(cm^3\ s)$, which corresponds to 0.3 pptv/h at atmospheric pressure. Given that values of a few pptv to tens of pptv of active bromine are required to be atmospherically significant, this simple calculation illustrates this chemistry may be important as not only an initiation step that precedes the autocatalytic $HOBr^-$ cycle but also as an active bromine source in its own right.

5. Summary

In this work we demonstrate that a heterogeneous reaction occurs between gas-phase OH and sodium halide solutions, to yield gas-phase Br_2. Cl_2 is only formed when the bromide levels in solution are sufficiently depleted. Given the rapid interactions that occur between OH and both Cl^- and Br^- in solution, it is likely that the chemistry occurs at the surface of these solutions, even in the absence of any partitioning of halides to the surface. Indeed, bulk chemistry can explain the very strong preference for oxidation of bromide over chloride. However, it cannot explain the observed pH dependence of the bromine production rates in the concentrated CSB solutions, suggestive that interfacial chemistry is occurring differently from that in the bulk. The strong acidity dependence of the bromine yields indicate that this chemistry will be most important in air that has been subjected to anthropogenic influence. We show that this process may be viable as a source of active bromine in the atmosphere, although future work remains to better assess its significance relative to other sources. Our finding that a surface coating of an organic surfactant, SDS, significantly reduces bromine production reinforces the need to better determine the degree to which such coatings exist on atmospheric particulates. This work clearly shows that an organic surfactant can significantly affect the rate of interfacial mass transfer of OH radicals to an aqueous aerosol.

In the future, we intend to extend these studies to the formation of Br_2 from solid surfaces, such as snow and ice that contain halides, as well as to solid salts. We believe the former needs to be investigated in order to determine the potential of this chemistry as a bromine source in the polar boundary layer, where active bromine levels are observed to increase with polar sunrise. Similarly, the chemistry on solid salts may be important in salt lake environments.

Acknowledgment. This work was funded by NSERC. We thank Ingrid George and Cort Anastasio for showing us a preprint of their work prior to publication and for help with the numerical model of solution chemistry.

References and Notes

(1) Foster, K. L.; Plastridge, R. A.; Bottenheim, J. W.; Shepson, P. B.; Finlayson-Pitts, B. J.; Spicer, C. W. *Science* **2001**, *291*, 471.
(2) Platt, U.; Hönninger, G. *Chemosphere* **2003**, *52*, 325.
(3) Sander, R.; Crutzen, P. J. *J. Geophys. Res.* **1996**, *101*, 9121.
(4) Tas, E.; Peleg, M.; Matveev, V.; Zingler, J.; Luria, M. *J. Geophys. Res.* **2005**, *110*, doi: 10.1029/2004JD005665.
(5) Vogt, R.; Crutzen, P. J.; Sander, R. *Nature* **1996**, *383*, 327.
(6) von Glasow, R.; von Kuhlmann, R.; Lawrence, M. G.; Platt, U.; Crutzen, P. J. *Atmos. Chem. Phys.* **2004**, *4*, 2481.
(7) Barrie, L. A.; Bottenheim, J. W.; Schnell, R. C.; Crutzen, P. J.; Rasmussen, R. A. *Nature* **1988**, *334*, 138.
(8) Abbatt, J. P. D.; Nowak, J. B. *J. Phys. Chem. A* **1997**, *101*, 2131.
(9) Fan, S.-M.; Jacob, D. J. *Nature* **1992**, *359*, 522.
(10) Newberg, J. T.; Matthew, B. M.; Anastasio, C. *J. Geophys. Res.* **2005**, *110*, doi: 10.1029/2004JD005446.
(11) Pszenny, A. A. P.; Moldanová, J.; Keene, W. C.; Sander, R.; Maben, J. R.; Martinez, M.; Crutzen, P. J.; Perner, D.; Prinn, R. G. *Atmos. Chem. Phys.* **2004**, *4*, 147.
(12) Simpson, W. R.; Alvarez-Aviles, L.; Douglas, T. A.; Sturm, M.; Domine, F. *Geophys. Res. Lett.* **2005**, *32*, doi: 10.1020/2004GL021748.
(13) Toom-Sauntry, D.; Barrie, L. A. *Atmos. Environ.* **2002**, *36*, 2683.
(14) Oum, K. W.; Lakin, M. J.; DeHaan, D. O.; Brauers, T.; Finlayson-Pitts, B. J. *Science* **1998**, *279*, 74.
(15) Finlayson-Pitts, B. J.; Livingston, F. E.; Berko, H. N. *Nature* **1990**, *343*, 622.
(16) Mozurkewich, M. *J. Geophys. Res.* **1995**, *100*, 14199.
(17) George, I. J.; Anastasio, C. *Atmos. Environ.*, to be submitted for publication.
(18) Matthew, B. M.; George, I.; Anastasio, C. *Geophys. Res. Lett.* **2003**, *30*, doi: 10.1029/2003GL018572.
(19) Zafiriou, O. C. *J. Geophys. Res.* **1974**, *79*, 4491.
(20) Herrmann, H.; Majdik, Z.; Ervens, B.; Weise, D. *Chemosphere* **2003**, *52*, 485.
(21) Matheson, M. S.; Mulac, W. A.; Weeks, J. L.; Rabani, J. *J. Phys. Chem.* **1966**, *70*, 2092.
(22) Zehavi, D.; Rabani, J. *J. Phys. Chem.* **1972**, *76*, 312.

(23) Hanson, D. R.; Burkholder, J. B.; Howard, C. J.; Ravishankara, A. R. *J. Phys. Chem.* **1992**, *96*, 4979.
(24) Ghosal, S.; Shbeeb, A.; Hemminger, J. C. *Geophys. Res. Lett.* **2000**, *27*, 1879.
(25) Roeselová, M.; Jungwirth, P.; Tobias, D. J.; Gerber, R. B. *J. Phys. Chem. B* **2003**, *107*, 12690.
(26) Roeselová, M.; Vieceli, J.; Dang, L. X.; Garrett, B.; Tobias, D. J. *J. Am. Chem. Soc.* **2004**, *126*, 16308.
(27) Zangmeister, C. D.; Turner, J. A.; Pemberton, J. E. *Geophys. Res. Lett.* **2001**, *28*, 995.
(28) Hanson, D. R.; Lovejoy, E. R. *J. Phys. Chem.* **1996**, *100*, 6397.
(29) Cziczo, D. J.; Abbatt, J. P. D. *J. Phys. Chem. A* **2000**, *104*, 2038.
(30) Rockland, L. B. *Anal. Chem.* **1960**, *32*, 1375.
(31) Bertram, A. K.; Ivanov, A. V.; Hunter, M.; Molina, L. T.; Molina, M. J. *J. Phys. Chem. A* **2001**, *105*, 9415.
(32) Huey, L. G.; Hanson, D. R.; Howard, C. J. *J. Phys. Chem.* **1995**, *99*, 5001.
(33) Thornton, J. A.; Braban, C. F.; Abbatt, J. P. D. *Phys. Chem. Chem. Phys.* **2003**, *5*, 4593.
(34) Arnold, S. T.; Viggiano, A. A. *J. Phys. Chem. A* **2001**, *105*, 3527.
(35) Howard, C. J. *J. Phys. Chem.* **1979**, *83*, 3.
(36) DeMore, W. B.; Sander, S. P.; Golden, D. M.; Hampson, R. F.; Kurylo, M. J.; Howard, C. J.; Ravishankara, A. R.; Kolb, C. E.; Molina, M. J. *JPL Publ.* **1997**, *97-4*.
(37) Ershov, B. G.; Kelm, M.; Gordeev, A. V.; Janata, E. *Phys. Chem. Chem. Phys.* **2002**, *4*, 1872.
(38) Finlayson-Pitts, B. J. *Chem. Rev.* **2003**, *103*, 4801.
(39) Ellison, G. B.; Tuck, A. F.; Vaida, V. *J. Geophys. Res.* **1999**, *104*, 11633.
(40) Gill, P. S.; Graedel, T. E.; Weschler, C. J. *Rev. Geophys.* **1983**, *21*, 903.
(41) Chatterjee, A.; Moulik, S. P.; Sanyal, S. K.; Mishra, B. K.; Puri, P. M. *J. Phys. Chem. B* **2001**, *105*, 12823.
(42) Thomas, J. L.; Jimenez-Aranda, A.; Finlayson-Pitts, B. J.; Dabdub, D. *J. Phys. Chem. A* **2006**, *110*, 1859.
(43) Hanson, D. R.; Ravishankara, A. R.; Solomon, S. *J. Geophys. Res.* **1994**, *99*, 3615.
(44) Neta, P.; Huie, R. E.; Ross, A. B. *J. Phys. Chem. Ref. Data* **1988**, *17*, 1027.
(45) Petersen, P. B.; Saykally, R. J. *J. Phys. Chem. B* **2005**, *109*, 7976.
(46) Grigorev, A. E.; Makarov, I. E.; Pikaev, A. K. *High Energy Chem.* **1987**, *21*, 99.
(47) Cooper, P. L.; Abbatt, J. P. D. *J. Phys. Chem.* **1996**, *100*, 2249.
(48) Badger, C. L.; George, I. J.; Griffiths, P. T.; Abbatt, J. P. D.; Cox, R. A. *J. Phys. Chem. A* **2006**, *110*, 6986.
(49) McNeill, V. F.; Patterson, J.; Wolfe, G. M.; Thornton, J. A. *Atmos. Chem. Phys. Discuss.* **2006**, *6*, 17.
(50) Thornton, J. A.; Abbatt, J. P. D. *J. Phys. Chem. A* **2005**, *109*, 10004.
(51) Hunt, S. W.; Roeselová, M.; Wang, W.; Wingen, L. M.; Knipping, E. M.; Tobias, D. J.; Dabdub, D.; Finlayson-Pitts, B. J. *J. Phys. Chem. A* **2004**, *108*, 11559.